scientific reports

OPEN

Heatwaves amplify air pollution risks in Sub-Saharan Africa

Egide Kalisa[1] & Andrew Sudmant[2]

Mounting evidence demonstrates that heatwaves aggravate urban air pollution, with substantial impacts on public health, but comparatively little research has addressed Sub-Saharan African contexts. In this study, we focused on Kigali, Rwanda, to assess the relationship between extreme heat events and concentrations of fine particulate matter ($PM_{2.5}$), nitrogen dioxide (NO_2), and ozone (O_3) from 2021 to 2024. Using low-cost sensors for dense spatiotemporal coverage, our analysis finds that O_3 concentrations increased significantly during 6 heatwave events with peak values up to 40% higher during heatwaves. Heatwaves also resulted in spikes in $PM_{2.5}$ and NO_2, however the diurnal and seasonal analyses showed that $PM_{2.5}$ and NO_2 dynamics were shaped more by local emissions than temperature alone. These results highlight the compound risks of heat and air pollution in sub-Saharan African cities, underscoring the importance of early-warning systems and robust urban policies that account for both heat and air pollution. In addition, the atmospheric dynamics identified in this research differ from those observed in many high-income countries, highlighting a critical need for more research exploring the intersection of heat and air pollution in Sub-Saharan Africa.

Keywords Heatwave, Ozone, Particulate matter, Nitrogen dioxide, Sub-Saharan Africa

Heatwaves are occurring with increasing frequency and severity worldwide, primarily driven by anthropogenic climate change[1,2]. These extreme temperature events amplify air pollution through intensified photochemical reactions leading to higher ozone (O_3) formation, and by creating stagnant atmospheric conditions that trap pollutants near ground level[3]. Multiple large-scale studies confirm that heat and air pollution jointly produce greater health risks than either hazard alone. For instance, a recent global analysis of 620 cities demonstrated that the association between ambient air pollution exposure and mortality is modified by high ambient temperatures[4].

Similar compound effects have been observed in California, where extreme heat and $PM_{2.5}$ co-occurring on the same days nearly doubled mortality risk compared to the sum of their individual impacts[5]. In Seoul, heatwaves substantially boosted O_3 and fine particulate pollution ($PM_{2.5}$), though the patterns for nitrogen dioxide (NO_2) and coarse particulate pollution (PM_{10}) varied depending on meteorological conditions[6]. Urban centres in China have seen a steep rise in days combining extreme heat and high O_3, driving up total population exposure to "compound extremes"[7]. Power plants in India and China emit surges of sulphur dioxide (SO_2) and NO_2 during heatwaves due to soaring electricity demand in a feedback loop that worsens local smog right when populations are already heat-stressed[8].

Evidence of compound heat–pollution risks extend beyond mortality to encompass broader health outcomes. In California, co-exposure to extreme heat and elevated pollutants has been linked to preterm birth risks[9]while in China, hypertension incidence among older adults rises disproportionately when heatwaves coincide with $PM_{2.5}$ spikes, especially in neighbourhoods lacking green spaces[10]. Research in China has also found that the risk of dying from cardiovascular and respiratory causes during concurrent heatwaves and elevated O_3[11]. Together, these findings confirm that climate change is intensifying the co-occurrence of extreme heat and polluted air, creating compound hazards that disproportionately threaten vulnerable populations including the elderly, pregnant individuals, and those with preexisting health conditions.

While a growing body of research considering contexts in Europe, North America, and parts of Asia, sub-Saharan Africa (SSA) remains underrepresented in literature considering air pollution and public heath[4]. When African contexts appear, they tend to be limited in geographic scope (often including only a few South African cities) or treat temperature as a background variable rather than a catalyst that can directly drive air pollution levels[12,13]. This gap persists even as SSA undergoes rapid urbanization, grapples with growing industrial emissions, biomass burning, and natural dust intrusions and faces rising urban temperatures. For instance, a 2024 Nigerian heatwave dust event underscored how local factors (Saharan dust) can merge with extreme heat to cause severe air quality deterioration[14]. Similar conditions could manifest elsewhere on the continent,

[1]Department of Epidemiology and Biostatistics, Schulich School of Medicine and Dentistry, Western University, London, ON N6G 2M1, Canada. [2]Edinburgh Climate Change Institute, University of Edinburgh, High School Yards, Edinburgh, UK. ✉email: ekalisa2@uwo.ca

particularly in fast-growing cities with strained infrastructure, limited air quality monitoring, and rapidly increasing demand for energy[8].

Recent studies demonstrate that low-cost air quality sensors can help to bridge critical air quality monitoring gaps in sub-Saharan African cities by providing high-resolution spatiotemporal data[15–17]. For example, pilot sensor networks in Kinshasa and Brazzaville captured annual $PM_{2.5}$ concentrations four to five times higher than WHO guidelines, and multiyear deployments in Lomé have shown seasonal spikes in pollution due to regional dust transport[17]. These examples highlight the potential of low-cost sensor networks to augment environmental data collection for climate-related air pollution research in data-scarce regions and the degree to which air quality risks in SSA may be an underappreciated risk to public health and well-being.

Kigali, the capital of Rwanda, offers a case that could help to advance understanding of compound urban heat and air pollution risks in a Sub-Saharan African context. As one of the fastest urbanizing cities in SSA[18]Kigali faces emerging threats from extreme heat events, high background pollution from vehicle traffic and biomass burning, and limited capacity for comprehensive environmental monitoring. The core processes behind heatwave–pollution interactions, production of pollutants (especially O_3 and secondary aerosols), reduced atmospheric mixing under stagnant high-pressure systems, and potential spikes in local emissions during hot periods are therefore found in Kigali[5,6].

This study has four main objectives. First, it quantifies changes in $PM_{2.5}$, NO_2, and O_3 concentrations in Kigali during heatwave versus non-heatwave days. Second, it assesses the role of seasonality (comparing the dry and wet seasons) in modifying how extreme heat affects pollution levels. Third, it examines how humidity and air stagnation mediate pollution concentrations during heatwave episodes, shedding light on the meteorological underpinnings of these events in a tropical highland environment. Finally, this study discusses policy implications, particularly around integrating heatwave alerts with air quality advisories to safeguard public health.

Methods

Study area and data sources

Rwanda is a landlocked country in Sub-Saharan Africa, with a high population density (503 people per square kilometre in 2022), which is the second highest in Africa after Mauritius. Rwanda has two main seasons (dry and wet) and experiences a tropical climate with air temperatures between 16 °C and 20 °C. Due to its high altitude, Rwanda experienced only rare heatwaves historically. However, some valleys and urban basins in Kigali, the capital of Rwanda, can trap heat due to weather inversion. Further, the 1994 genocide created widespread environmental degradation that has made the Rwandan population vulnerable to extreme climate weather events such as heatwaves. In the last 30 years, Rwanda has undergone rapid urbanization, population growth, and urban expansion. This has created urban heat islands in larger cities as a result of high-density building and reductions in vegetative cover. Rwanda also experiences periods of low wind speeds and little rainfall, especially during the dry season, and the Eastern region experiences El Niño events, causing droughts and floods in the East and Western provinces of the country. Consequently, air quality during heatwaves in Rwanda may vary considerably, especially in Kigali City, the largest city in Rwanda, which suffers from air pollution episodes[19–21].

This study analyzes $PM_{2.5}$, NO_2, and O_3 concentrations obtained from 12 air quality stations in Kigali from May 2021 to December 2024 (Fig. 1). These air quality stations are operated by the Human Environment, Location, Transport and Health (HELTH) Research Lab (https://egidekalisa.com/) and the Rwanda Environmental Management Authority (REMA) (https://aq.rema.gov.rw/). The hourly averaged pollutant concentrations were analysed along with meteorological data (daily minimum, mean and maximum temperatures, relative humidity) obtained from the Rwanda Meteorological Agency (https://www.meteorwanda.gov.rw).

Air pollution measurements and calibration

Real-time $PM_{2.5}$, NO_2 and O_3 data (measurements over 60 s) were collected at 12 sites (Fig. 1) in Kigali City using lower-cost, real-time, affordable multi-pollutant (RAMP) monitors from 2021 to 2024. The description and calibration of these RAMPs were published in our previous study in Rwanda[19,22] and detailed in a previous study[47]. The RAMP system (Sensit Technology, USA) units were located 2–3 m above the ground, using passive electrochemical sensors (Alphasense, UK) to measure three gases and particles (nitrogen dioxide (NO_2), ozone (O_3), particulate matter ($PM_{2.5}$) and meteorological parameters (temperature and relative humidity)[22,47]. These sensors collect raw signal data, which is then processed and averaged to produce 60-second air quality measurements. For local data verification in this study, we compared $PM_{2.5}$ data from 2021 to 2024 from RAMP to data for the same period obtained from a ground-monitored beta attenuation mass monitor (BAM) reference station operated by the US Embassy (https://www.airnow.gov/) in Kigali from 2022 to 2024. This BAM station is 5–10 km from our sampling sites and the Kigali reference air quality station. The correlation analysis showed that RAMP and BAM data correlated yearly ($R^2 > 0.6$, $P < 0.00$). The correlation analysis showed that BAM-$PM_{2.5}$ data were positively correlated with RAMP at 60%, suggesting some intra-urban variability associated with local activities, such as traffic.

Due to data availability, we did not perform local verification of NO_2 and O_3 for this study, however, our previous studies have conducted quality control and quality assurance using generalized RAMP (gRAMP) calibration models[22,47]. The RAMP low-cost sensors used for this study are subject to known cross-interference and environmental sensitivities. Electrochemical sensors are known to have temperature and relative humidity cross-interference issues, and O_2 is notorious for interfering with the detection of nitric oxide and NO_2. To address cross-interference between O_3 and NO_2, our previous study developed a calibration model. It co-located the RAMP with a reference monitor (Teledyne T400) that measures O_3 and NO_2[22]. Both these models and the co-located reference monitors were validated with independent data and demonstrate good performance for O_3. Furthermore, to minimize sensor-based environmental bias, we utilized temperature and relative humidity data obtained from the Rwanda Meteorological Agency. Additionally, the observed hourly variation in O_2 and NO_2

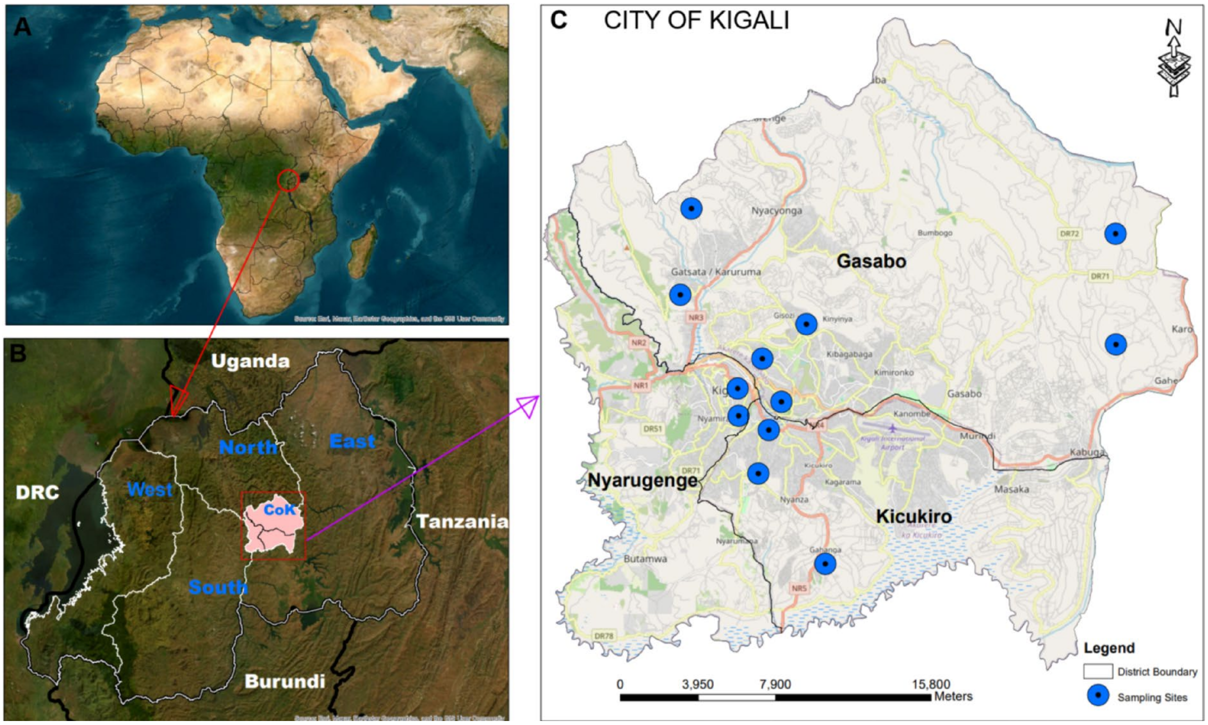

Fig. 1. Map of Africa (**A**) showing the geographic location of Rwanda and the city of Kigali (**B**). Map (**C**) shows the locations of the air quality monitoring stations (blue circles). *Source*: The satellite imagery was obtained using ArcGIS Desktop version 10.8 (Esri, Redlands, CA, USA) with the default "World Imagery" basemaps provided through ArcGIS Online. The imagery is sourced from ESRI, DigitalGlobal, GeoEYE, Earthstar Geographics and used following ESRI's terms of use for publications. https://www.esri.com/en-us/arcgis/products/arcgis-desktop/overview.

is consistent across various days and locations, indicating that these patterns represent genuine atmospheric processes rather than calibration or drifting artifacts.

Identifying heatwaves

No universally accepted heatwave definition exists, as climate norms vary widely between regions[23,48]. Our heatwave definition was based on existing literature[3]. We define a heatwave as three or more consecutive days exceeding the average daily maximum temperature by 5 °C, with the daily average determined for the period between 1961 and 1990[24]. From 2021 to 2024, the daily maximum temperature was 25.28 °C for Kigali. We identified six heatwaves with maximum temperatures of 32.3 –33.5 °C. We also defined non-heatwaves periods as days with temperatures below the 90th percentile threshold and not meeting our heatwave definition[23]. Our heatwave definition may appear moderate compared to the definitions used in temperate regions. However, in Rwanda's high-altitude areas, including Kigali, the daily maximum temperature can be lower than 16–20 °C. Thus, a sudden increase above 32 °C represents almost 12–16 °C above normal and may lead to thermal stress and health impacts. Our definition aligns with approaches to heatwave identification in several countries in East Africa, such as Uganda, and countries in Asia, such as Vietnam and Thailand, with similar baseline climates and topographies. For example, the neighbouring country of Uganda has reported heat-related health warnings in Kampala city at 30–33°C[49], while Vietnam[50] considers heatwaves to be temperatures of 32–35 °C for 2 to 3 consecutive days.

Results

Descriptive analysis

Concentrations of $PM_{2.5}$, NO_2, and O_3 from 2021 to 2024 show different seasonal relationships (Table 1). The Wilcoxon–Mann–Whitney test showed that the annual means for NO_2 were higher in the dry seasons than in the wet seasons. In contrast, the annual averages for $PM_{2.5}$ and O_3 were higher in the wet than the dry seasons (Table 1). The diurnal analysis (Fig. 2) shows that $PM_{2.5}$ peaked during morning hours (6:00–9:00 AM) and evening rush hours (17:00–23:00 PM) and was higher during the wet seasons. O_3 peaked around midday (13:00 am -16:00 pm) in both dry and wet seasons, as expected due to photochemical activity (Fig. 2). The concentration of NO_2 was higher during dry seasons than wet seasons. The overall results indicate distinct seasonal dynamic for different pollutants in Kigali.

Pollutants	Dry season [*n* = 71996]	Wet season [*n* = 58707]	**p*-value
$PM_{2.5}$ [μg/m^3]	37.7 ± 21.2	47.0 ± 23.2	< 0.001
NO_2 [μg/m^3]	21.3 ± 6.8	20.2 ± 6.5	< 0.001
O_3 [PPB]	21.7 ± 15.3	22.5 ± 10.5	< 0.001
Temp [°C]	20.6 ± 3.9	20.8 ± 3.9	< 0.001
RH [%]	66.0 ± 12.4	58.1 ± 13.8	< 0.001
Pollutants	**Non-heatwave [*n* = 20912]**	**Heatwave [*n* = 690]**	***p-value**
$PM_{2.5}$ [μg/m^3]	41.4 ± 16.2	43.1 ± 13.9	< 0.001
NO_2 [μg/m^3]	15.1 ± 4.1	16.6 ± 5.2	< 0.001
O_3 [PPB]	21.5 ± 7.9	24.8 ± 8.3	< 0.001

Table 1. Comparison of annual mean and standard deviation (mean ± SD) of $PM_{2.5}$, NO_2, and O_3 concentrations between dry and wet seasons and during heatwave and non-heatwave days from 2021–2024. *The p-value indicates the presence of statistically differences among air pollutant concentrations based on the Wilcoxon test.

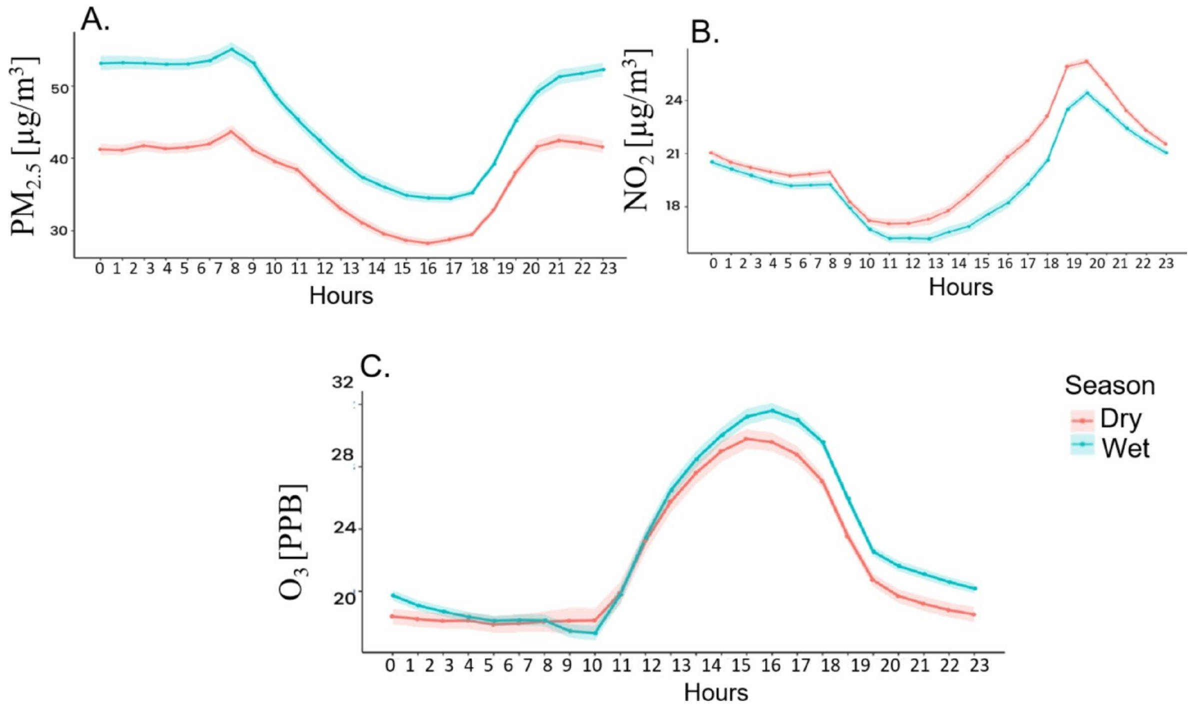

Fig. 2. Hourly variation of (**A**) $PM_{2.5}$, (**B**) NO_2, and (**C**) O_3 during both dry (red) and wet seasons (green).

Identification of heatwaves and associated air pollutant variation (2021–2024)

Examining all six heatwaves, the highest maximum temperature was observed in March 2022 but corresponded to lower concentrations of $PM_{2.5}$, O_3 and NO_2 relative to the other heatwave events. The most prolonged heatwaves, lasting five days, were observed in January 2022 and June 2023. Over the 4 years covered by the data in this study, the highest mean concentrations of $PM_{2.5}$ (55.6 (μg/m^3) and NO_2 (17.24 μg/m^3) coincided with heatwaves that involved five consecutive days with maximum temperatures above 32 °C in 2022 and 2023, respectively (Table 2). While $PM_{2.5}$ and O_3 showed variations peaking during the longest heatwave peaks, NO_2 remained relatively stable during high-intensity and long-duration heatwaves.

Figure 3 shows the variation in the mean concentrations of air pollutants ($PM_{2.5}$, O_3, NO_2) and temperatures during heatwaves from 2021 to 2024. Generally, O_3 and NO_2 concentrations on days with heatwaves were elevated, however, the $PM_{2.5}$ concentration did not always increase at the same time as temperatures, and peak concentrations were delayed (Fig. 3). In 2021, two short heatwaves were associated with a minor peak in $PM_{2.5}$ observed during or after the heatwave (Fig. 3). January 2022 was identified as the most prolonged and most intense heatwave, with five consecutive days where the temperature was consistently above 32 °C. A spike in $PM_{2.5}$ concentration (80 μg/m^3) was observed before the heatwave while O_3 gradually increased over the heatwave event (Fig. 3). Another heatwave of ~ 4 consecutive days was observed in March 2022 (Fig. 3) with the highest temperature reaching ~ 34 °C. This heatwave showed $PM_{2.5}$ and O_3 increases not coinciding with

Year	Month	Period	Max. temp [°C]	Mean $PM_{2.5}$ [µg/m³]	Mean NO_2 [µg/m³]	Mean O_3 [ppb]
2021	September	14th – 16th	33.20 ± 3.67	39.75 ± 5.31	16.84 ± 5.72	24.65 ± 8.47
2021	September	19th – 21st	32.78 ± 3.45	40.35 ± 16.24	16.05 ± 5.77	27.46 ± 9.47
2022	January	24th – 28th	32.65 ± 3.51	55.59 ± 11.81	17.24 ± 4.97	26.42 ± 7.95
2022	March	05th – 8th	33.47 ± 3.04	30.28 ± 8.16	15.89 ± 4.99	21.70 ± 7.46
2023	June	26th -30th	32.95 ± 3.55	41.93 ± 9.09	16.26 ± 5.11	23.94 ± 7.70
2023	July	9th -11th	32.36 ± 3.79	40.04 ± 8.17	16.41 ± 5.05	23.56 ± 8.52

Table 2. Heatwave periods with corresponding annual maximum temperatures and concentrations of air pollutants ($PM_{2.5}$, O_3, NO_2) identified from 2021 to 2024.

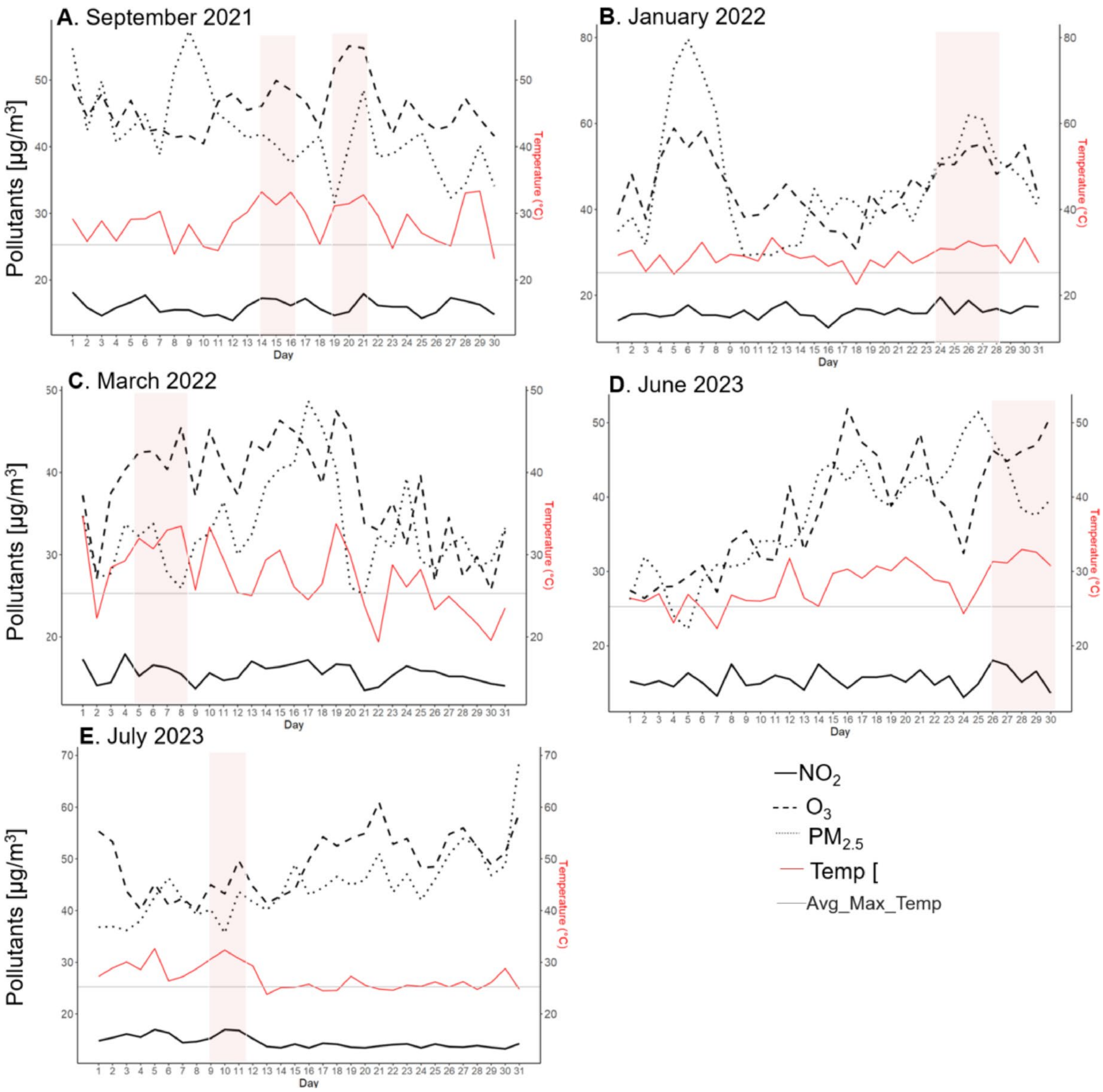

Fig. 3. Daily average concentrations of air pollutants ($PM_{2.5}$, NO_2 and O_3) and temperatures during heatwaves identified in Table 2. The shaded red color shows the heatwave period identified.

the heatwave but rising gradually after the heatwave. Another heatwave of 5 days was observed in June 2023 and showed levels of $PM_{2.5}$ and O_3 gradually increasing and peaking at the end of the heatwave (Fig. 3). O_3 levels showed an increase during and after heatwaves, with the highest concentration of 45 ppb observed after a heatwave. A moderate increase in NO_2 (~ 15 µg/m³) was also observed during heatwaves. These results indicated that O_3 was the most heatwave-responsive pollutant, consistently peaking during and after heatwaves, while $PM_{2.5}$ showed variable timings, with peaks before, during and after heatwaves. NO_2 showed less variation with heatwaves, suggesting it is emissions-driven.

Characteristics of pollutants during heatwave events

Figure 4 shows the diurnal variation in $PM_{2.5}$, NO_2 and O_3 during heatwaves and non-heatwaves. The concentration of $PM_{2.5}$ was consistently high during heatwaves, with a clear peaks in the morning (08:00 am -10:00 am), with pollution levels reaching around 64 μg/m^3, and decreases in the middle of the day (11:00–16:00) showing lower concentrations < 35 μg/m^3 during both heatwaves and non-heatwave events. O_3 showed the clearest response to heatwaves, increasing as the heatwaves increased, peaking during the middle of the day (10:00–16:00) and remaining elevated even after the end of the heatwaves in the evening (17:00–20:00). NO_2 showed noticeable peaks in the middle of the day (~ 2:00 pm) during heatwaves and remained higher during the evenings (6:00–7:00 pm) on heatwave days, while in the morning the concentration dropped, likely due to increased photochemical conversion to O_3.

The findings suggest that extended and intense heatwaves are associated with increased O_3 concentrations during and after heatwaves. In contrast, $PM_{2.5}$ and NO_2 did not increase uniformly or consistently. Although longer heatwaves resulted in high pollution peaks of $PM_{2.5}$ and NO_2, the diurnal and seasonal analyses suggest that $PM_{2.5}$ and NO_2 dynamics are shaped more by local emissions sources than temperature alone during heatwaves, as indicated by existing literature on air pollution sources in Rwanda and Kigali[19]. The observed peak in NO_2 levels during heatwave periods, particularly from 12:00 pm to 14:00 (Fig. 4C), aligns with photo-stationary state (PSS) dynamics, where increased levels of nitric monoxide (NO) titrate O_3 due to a temporal rise in NO_2 and a reduction in O_3. This interaction is plausible under heatwave conditions, which often involve precursor emissions and vertical mixing. The sharp dip in O_3 levels around 15:30 on heatwave days coincided with a lack of confidence interval shading (Fig. 4C), suggesting very limited or single data point coverage at that hour. Although the broader observed O_3 trend throughout the day remains consistent (Fig. 4C) and is well supported across hours with sufficient data, the drop dip observed in O_3 levels is likely an artifact rather than confirmed atmospheric events.

Correlation analysis of air pollution and heatwaves

Based on linear regression analysis, the relationship between $PM_{2.5,}$ NO_2, O_3, and temperature during all six heatwaves was identified for the period from 2021 to 2024 (Fig. 5). The results of the monthly trend from 2021 to 2024 show that both $PM_{2.5}$ and O_3 concentrations (Fig. 5A) consistently peak during the dry months (June-August), coinciding with lower relative humidity (Fig. 4B), while decreasing from March to May during the rainy season. For instance, Fig. 4B shows that $PM_{2.5}$ has an inverse relationship with relative humidity; i.e.,

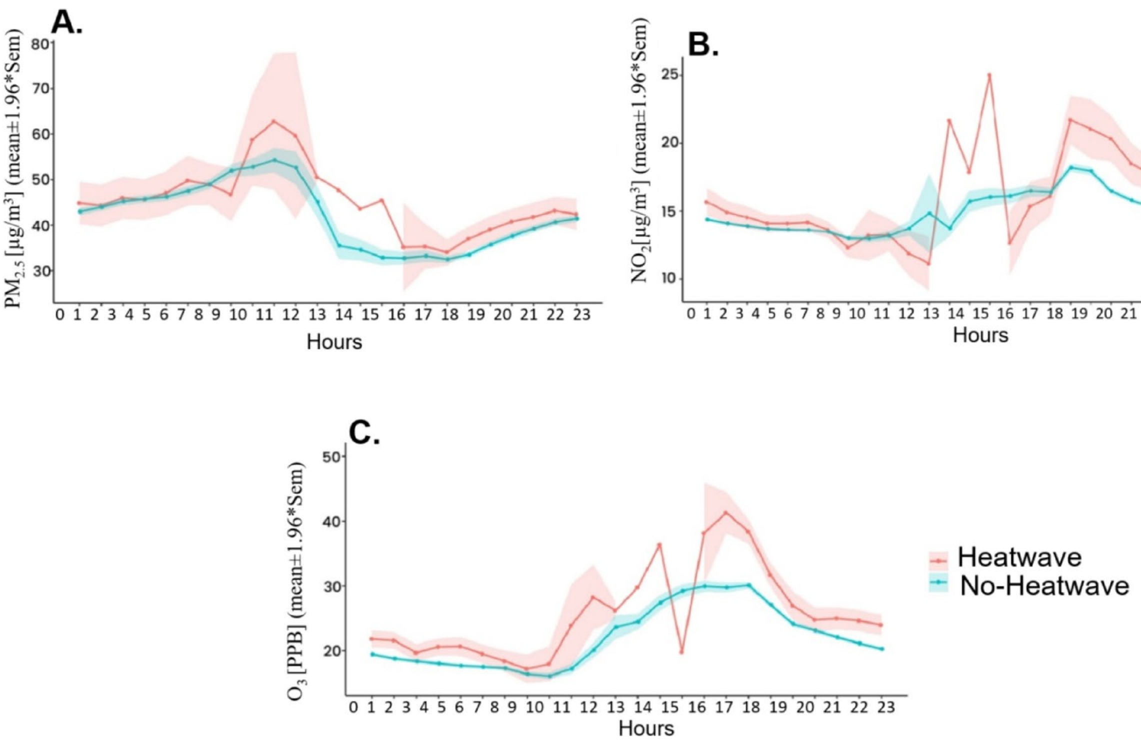

Fig. 4. Mean Hourly variation of $PM_{2.5}$, O_3, and NO_2 during heatwaves (Red color) and non-heatwaves (Green colour), averaged across all monitoring sites and stratified by hours. Data reflect measurements from January to December from 2021 to 2024 Shaded areas represent the 95% confidence interval (mean ± *1.96 x SEM*)). The absence of a shading area at some time points indicates limited valid observations.

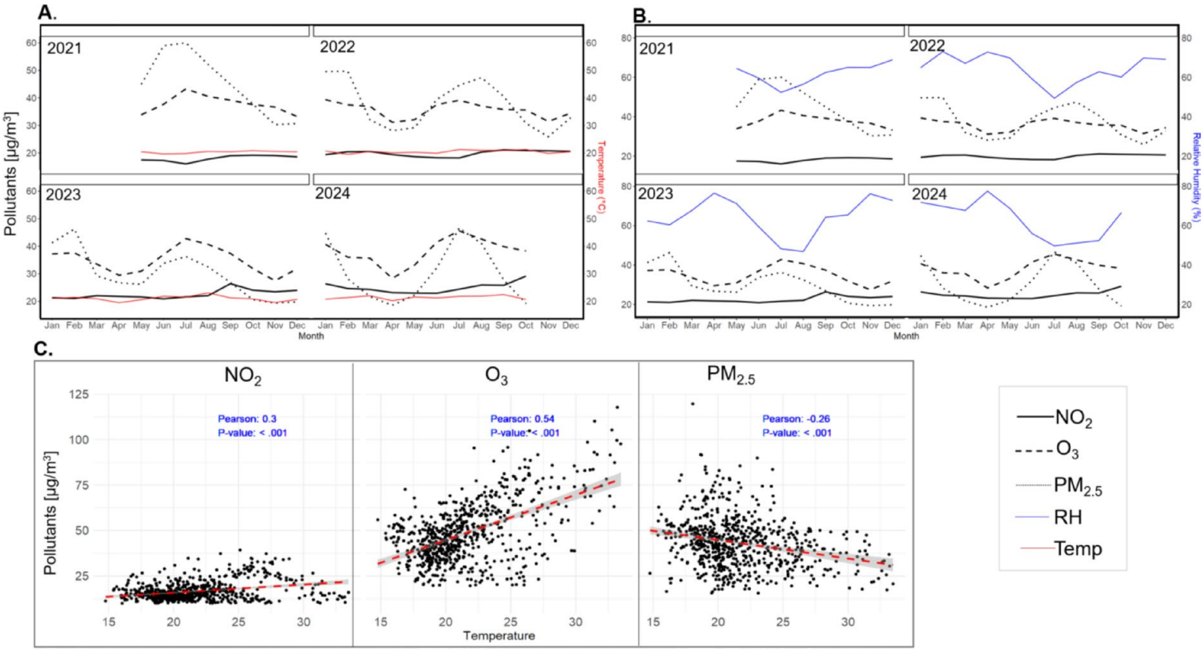

Fig. 5. (**A**) Monthly variation of ambient $PM_{2.5}$ (dashed black line), O_3 (dotted black line) and NO_2 concentration ((Solid black line),) and temperature (red line) from January 2021 to December 2024, (**B**) Monthly variation of ambient $PM_{2.5}$ (dashed black line), O_3 (dotted black line) and NO_2 concentration ((Solid black line),) and temperature (red line) from January 2021 to December and relative humidity (blue line) from January 2021 to December 2024; and (**C**) correlation analysis of air pollutants (PM_{10}, NO_2 and O_3) during heatwaves identified in 2021, 2022 and 2023.

as relative humidity increases above 50%, $PM_{2.5}$ levels decrease. A possible explanation is that humidity helps remove pollutants from the atmosphere through wet deposition and by forming larger particles that are more easily removed from the air. These results suggest that humidity enhances particle removal via washout or wet deposition of $PM_{2.5}$ while lower humidity favours the accumulation of air pollutants. Conversely, dry conditions can lead to less vertical mixing in the atmosphere, trapping pollutants closer to the ground and causing them to accumulate.

While NO_2 remains relatively stable throughout the year, $PM_{2.5}$ exhibits substantial seasonal variation, likely driven by biomass burning and road dust suspension during the dry season. O_3 concentrations increase with temperature, indicating the contribution of photochemical formation.

Figure 5C shows a correlation of O_3 with temperature (R^2 = 0.54, P < 0.001), confirming that elevated temperature during heatwaves may contribute to enhanced photochemical ozone formation, consistent with the results of seasonal variations in Fig. 4A. The relationship between O_3 and temperature is complex with other factors such as relative humidity, solar radiation, precursor concentrations (nitrogen oxides (NO_x), non-methane volatile organic compounds (NMVOCs), carbon monoxide (CO), methane (CH_4) playing a role. A positive correlation was also observed for NO_2 and temperature (R^2 = 0.30, P < 0.001), suggesting that NO_2 tends to increase with temperature. Conversely, $PM_{2.5}$ showed a negative correlation (R^2 = -0.26, P < 0.001), suggesting that elevated temperature may enhance vertical mixing and dispersion of $PM_{2.5}$, reducing ground concentrations. This negative relationship may be more complex than anticipated due to heightened convection and dilution at elevated temperatures, indicating the impact of increased atmospheric dispersion or decreased biomass burning during warmer periods.

Discussion

In the last 30 years, Rwanda has undergone rapid urbanization, population growth, and urban expansion. This rapid development has led to the creation of urban heat islands in larger cities, driven by high-density building and reductions in vegetation coverage, and increased air pollution due to the continued use of biomass for cooking and the growing number of vehicles for transport.

Alongside these meteorological extremes brought by El Niño events, Rwanda has experienced an average temperature increase of 1.4 °C in recent decades, with projections of reaching 2 °C by 2030[25]. Heatwaves under these conditions can exacerbate health impacts of air pollution, notably increasing respiratory and cardiovascular stress among vulnerable populations. Similar issues have been documented worldwide, where both heatwaves and air pollution are linked to greater climate instability and higher mortality[3,10,11]particularly in vulnerable populations[11]. Continued heatwaves and air pollution are expected to lead to greater climate instability[26,23]. Sub-Saharan Africa experiences high levels of air pollution influenced by urbanization, traffic emissions, biomass burning, wildfires, and industrial activities, and it is one of the regions that is expected to be most affected by climate change[1].

Our analysis reveals that $PM_{2.5}$ concentrations in both heatwave and non-heatwave periods often exceed the annual WHO air quality guidelines (5 μg/m^3) in Kigali, with levels occasionally reaching more than eight times the recommended thresholds due to rapid urbanization, dust emissions, emissions from old diesel vehicles, and agricultural fires[19–21,27,28]. In contrast, O_3 and NO_2 generally fell within annual WHO limits (60 μg/m^3 and 10 μg/m^3), respectively, but displayed notable spikes during both heatwaves and non-heatwave periods. Surprisingly, $PM_{2.5}$ peaked during the wet season, which deviates from global trends and points due to the role of Rwanda's mountainous topography in retaining pollutants at ground level. High humidity further promotes aerosol formation and can interact with biomass burning emissions, potentially contributing to prolonged pollution episodes[20,29].

We also observed that extended heatwaves drive up O_3 and $PM_{2.5}$ concentrations, whereas NO_2 levels were more strongly tied to local emissions than temperature alone. Correspondingly, daily "rush-hour" peaks in NO_2 and $PM_{2.5}$ were detected in the morning and evening, and overnight emissions of $PM_{2.5}$ often accumulated under low boundary-layer heights. Pearson correlation analyses underscores positive relationships between heatwaves and both O_2 and NO_2, while $PM_{2.5}$ exhibited a negative correlation—indicating that $PM_{2.5}$ can reach high levels even after heatwave conditions start to subside, reflecting the complex atmospheric dynamics in sub-Saharan Africa. These findings collectively emphasize the need for improved air quality monitoring networks and specialized early warning systems to address pollution spikes during and after prolonged heatwaves.

These findings underscore the need for a comprehensive approach to managing heatwaves and air pollution in African cities, a need that will grow more critical with continued urban growth and global warming. Policies have been established to protect the general public from heatwaves and air pollution, with heat warnings and air quality alerts in place in many wealthy nations[30–32]but these protections are not currently available in much of Africa, where many cities lack sufficient long-term air quality monitoring and early warning systems to take targeted actions to protect the health of their citizens. Coordinated efforts from meteorological agencies, health authorities, and local governments, and communication to the public via text-based advisories and public service announcements, could alert residents to imminent risks and recommend protective measures[33]. Lessons can be drawn from initiatives like the Freetown Heat Action Plan, which provides community-focused strategies and creates "cool zones" for vulnerable populations[34]. Implementing similar programs may help to reduce heat-related illnesses and limit exposure to pollution spikes during extreme weather events.

Cost-effective and easily deployable sensors can strengthen air quality surveillance in regions with limited resources. Real-time data on pollution hotspots, particularly during and immediately after heatwaves, would allow authorities to target interventions, such as traffic restrictions or intensified enforcement of emissions regulations. Community-based sensors can also raise public awareness and foster local ownership of air quality and climate initiatives[35].

Addressing the dual challenges of urban heat and air pollution also requires policies that link climate resilience with emission reductions. In many African cities, soaring temperatures caused by the urban heat island effect are compounded by air pollution from traffic, industry, and inefficient energy use, trends that are intensified by rapid urbanization[36].The most vulnerable communities, especially those in informal settlements, face disproportionate health risks due to inadequate housing, limited cooling options, and under-recognized exposure to extreme heat[37].

One promising avenue involves implementing nature-based solutions (NbS), such as urban tree planting, wetland restoration, and green roofing, which can simultaneously lower temperatures and filter pollutants[38]. By thoughtfully selecting tree species to avoid high biological VOC emissions, and integrating cleaner technologies (e.g., electric transit systems), cities can address the root causes of both heat and pollution[39,40]. Moreover, stronger regulatory frameworks including tightened vehicle emission standards or industrial air quality controls can ensure that pollution-related hazards are minimized while also advancing climate goals[41].

Coordinating urban planning and policy across sectors yields the greatest benefits, as evidenced by studies showing that aggressive emission cuts avert thousands of premature deaths related to fine particulate matter and O_3 exposure[42]. Cities such as Nairobi and Lagos have begun integrating climate resilience strategies into broader development plans, adopting clean energy and sustainable transport initiatives to achieve both climate and health co-benefits[43]. Fundamentally, aligning air quality management with climate adaptation and mitigation not only safeguards public health but also fosters more resilient, livable urban environments[19,21,44].

Several limitations of this study are important to highlight. This study was constrained by a relatively short-term dataset covering only four years (2021–2024), collected from 12 sites in Kigali. Although these measurements provide valuable insights into heatwave–pollution interactions in a Sub-Saharan African context, the data may not fully capture long-term or interannual climate–pollution dynamics. Extending both the duration of monitoring and the number of sites would allow for more robust statistical analyses and a better understanding of how climatic trends over time influence air quality patterns in rapidly urbanizing regions.

A second limitation involves the use of low-cost sensors. These sensors perform better at measuring particles than gases. Consequently, at this stage of development, the data collected for gases may be less reliable than that for particulates. While these devices were calibrated against a Beta Attenuation Mass Monitor (BAM) station and demonstrated strong correlations ($R > 0.60$, $p < 0.001$), uncertainties remain due to inherent sensor variability and the limited availability of reference-grade monitors in the region. $PM_{2.5}$ data calibration was performed with annual correlation with the BAM reference monitor situated at 5–10 km, highlighting the limitation of spatial representativeness for $PM_{2.5}$ that was assumed based on city-scale homogeneity without side-by-side direct correction analysis with the reference site. Additional reference sites, as well as standardized protocols for sensor calibration, could help refine data quality and improve comparability among different locations and time periods.

In addition, the meteorological data considered in this study included only temperature and relative humidity. Other factors, such as wind speed, solar radiation, nitrogen oxides (NO_x), volatile organic compounds (VOCs), boundary-layer height, and atmospheric pressure, also play essential roles in determining pollutant dispersion and the photochemical processes that lead to elevated O_2. More generally, combining low-cost sensor data with other sources of meteorological, economic, social and land-use data may be a promising approach for future research.

Finally, while this work illustrates how heatwaves can exacerbate air pollution, it does not include data on specific pollution sources or direct health outcomes. Understanding whether $PM_{2.5}$, NO_2, or O_2 originate from traffic, biomass burning, industry, or dust storms, and how these pollutants affect cardiovascular or respiratory health, would strengthen the evidence base for targeted interventions. Studies that integrate robust source apportionment techniques alongside epidemiological data would enable more accurate assessments of risk and the design of tailored mitigation strategies, especially for vulnerable populations.

Looking ahead, longer-term monitoring campaigns with broader geographic coverage, and enhanced meteorological data will help fill current gaps in knowledge. By linking air pollution data to health surveillance records, researchers can quantify the real-world impacts of compound hazards and guide resource allocation for public health interventions. This information, used to inform interdisciplinary efforts involving urban planners, policymakers, and public health practitioners are essential to address the growing challenges posed by rapid urbanization, climate variability, and limited monitoring infrastructure in Sub-Saharan African cities.

Data availability

All data are available upon reasonable request from the corresponding author (Egide Kalisa, email: ekalisa2@uwo.ca).

Received: 31 March 2025; Accepted: 15 July 2025
Published online: 21 July 2025

References

1. Intergovernmental Panel on Climate Change (IPCC). Climate Change 2021: The Physical Science Basis. Contribution of Working Group I to the Sixth Assessment Report of the Intergovernmental Panel on Climate Change. (2021). https://www.ipcc.ch/report/ar6/wg1//.
2. World Meteorological Organization (WMO). State of the Global Climate 2022. https://wmo.int/publication-series/state-of-global-climate-2022.
3. Kalisa, E., Fadlallah, S., Amani, M., Nahayo, L. & Habiyaremye, G. Temperature and air pollution relationship during heatwaves in Birmingham, UK. *Sustain. Cities Soc.* **43**, 111–120 (2018).
4. Stafoggia, M. et al. Joint effect of heat and air pollution on mortality in 620 cities of 36 countries. *Environ. Int.* **181**, 108258 (2023).
5. Rahman, M. M. et al. The effects of coexposure to extremes of heat and particulate air pollution on mortality in California: Implications for climate change. *Am. J. Respir. Crit. Care Med.* **206**, 1117–1127 (2022).
6. Park, K., Jin, H. G. & Baik, J. J. Do heat waves worsen air quality? A 21-year observational study in Seoul, South Korea. *Sci. Total Environ.* **884**, 163798 (2023).
7. Su, J., Jiao, L. & Xu, G. Intensified exposure to compound extreme heat and Ozone pollution in summer across Chinese cities. *npj Clim. Atmos. Sci.* **8**, 78 (2025).
8. Liu, S. et al. Underappreciated emission spikes from power plants during heatwaves observed from space: Case studies in India and China. *Earths Future*. **12**, e2023EF003937 (2024).
9. Sun, Y. et al. Examining the joint effects of heatwaves, air pollution, and green space on the risk of preterm birth in California. *Environ. Res. Lett.* **15**, 104099 (2020).
10. Zhou, W. et al. Combined effects of heatwaves and air pollution, green space and blue space on the incidence of hypertension: A National cohort study. *Sci. Total Environ.* **867**, 161560 (2023).
11. Du, H. et al. Exposure to concurrent heatwaves and Ozone pollution and associations with mortality risk: A nationwide study in China. *Environ. Health Perspect.* **132**, 047012 (2024).
12. Global Heat Health Information Network. Nigeria heatwave–dust event. Retrieved from https://ghhin.org (2024).
13. Gualtieri, G. et al. Potential of low-cost PM monitoring sensors to fill monitoring gaps in areas of Sub-Saharan Africa. *Atmos. Pollut Res.* **15**, 102158 (2024).
14. Bittner, A. S. et al. Performance characterization of low-cost air quality sensors for off-grid deployment in rural Malawi. *Atmos. Meas. Tech.* **15**, 3353–3376 (2022).
15. Raheja, G. et al. A network of field-calibrated low-cost sensor measurements of $PM_{2.5}$ in lomé, togo, over one to two years. *ACS Earth Space Chem.* **6**, 1011–1021 (2022).
16. World Bank. Concept Project Information Document (PID)—Rwanda Urban Mobility Project. http://documents.worldbank.org/curated/en/099350412232221350 (2022).
17. Kalisa, E., Sudmant, A., Ruberambuga, R. & Bower, J. Natural experiments in urban air quality: Lessons from car-free days and COVID-19 lockdowns in Kigali, Rwanda. *Cities Health* 1–12. https://doi.org/10.1080/23748834.2025.2468017 (2025).
18. Kalisa, E. et al. Characterization and risk assessment of atmospheric $PM_{2.5}$ and PM_{10} particulate-bound PAHs and NPAHs in Rwanda, Central-East Africa. *Environ. Sci. Technol.* **52**, 12179–12187 (2018).
19. Subramanian, R. et al. Air pollution in kigali, rwanda: Spatial and Temporal variability, source contributions, and the impact of car-free sundays. *Clean. Air J.* **30**, 1–15 (2020).
20. DeWitt, H. L. et al. Seasonal and diurnal variability in O_3, black carbon, and CO measured at the Rwanda Climate Observatory. *Atmos. Chem. Phys.* **19**, 2063–2078 (2019).
21. Government of Canada. Heat warning and information system harmonization. https://www.canada.ca/en/environment-climate-change/news/2016/05/heat-warning-and-information-system-harmonization.html (2016).
22. Atuyambe, L. M. et al. The health impacts of air pollution in the context of changing climate in africa: A narrative review with recommendations for action. *Ann. Glob. Health* **90**, 76 (2024).
23. Meehl, G. A. et al. An introduction to trends in extreme weather and climate events: Observations, socioeconomic impacts, terrestrial ecological impacts, and model projections. *Bull. Am. Meteorol. Soc.* **81**, 413–416 (2000).
24. Kalisa, E. & Adams, M. Population-scale COVID-19 curfew effects on urban black carbon concentrations and sources in Kigali, Rwanda. *Urban Clim.* **46**, 101312 (2022).
25. Malings, C. et al. Development of a general calibration model and long-term performance evaluation of low-cost sensors for air pollutant gas monitoring. *Atmos. Meas. Tech.* **12**, 903–920 (2019).

26. Li, C., Wei, W., Chan, P. W. & Huang, J. Heatwaves in Hong Kong and their influence on pollution and extreme precipitation. *Atmos. Res.* **315**, 107845 (2025).
27. Irankunda, E. et al. The comparison between in-situ monitored data and modelled results of nitrogen dioxide (NO_2): Case-study, road networks of Kigali City. *Rwanda Heliyon* **8**, e12390 (2022).
28. Kalisa, E., Kuuire, V. & Adams, M. Children's exposure to indoor and outdoor black carbon and particulate matter air pollution at school in rwanda, Central-East Africa. *Environ. Adv.* **11**, 100334 (2023).
29. US EPA. New York City Adapts To Deal with Projected Increase of Heat Waves. https://www.epa.gov/arc-x/new-york-city-adapts-deal-projected-increase-heat-waves#:~:text=In%20order%20to%20adapt%20to,future%20projected%20extreme%20heat%20events.
30. Ha, P. T. et al. Heatwaves in vietnam: Characteristics and relationship with large-scale climate drivers. *Int. J. Climatol.* **43**, 123–140 (2024).
31. United Nations Development Programme. Updated Nationally Determined Contribution (NDC) Mitigation and Adaptation Priorities for Rwanda. https://climatepromise.undp.org/s.
32. Grigorieva, E. & Lukyanets, A. Combined effect of hot weather and outdoor air pollution on respiratory health. *Lit. Rev. Atmos.* **12**, 790 (2021).
33. NOAA. National Integrated Heat Health Information System (NIHHIS). https://www.heat.gov/ (2025).
34. Wright, C. Y. et al. Climate change and human health in Africa in relation to opportunities to strengthen mitigating potential and adaptive capacity: Strategies to inform an African brains trust. *Ann. Glob Health* **90**, 7 (2024).
35. Freetown City Council. Trees, women and data: Early lessons from Freetown's Heat Action Plan. https://www.climateresilience.org/freetown-heat-action-plan-lessons (2023).
36. Manshur, T. et al. A citizen science approach for air quality monitoring in a Kenyan informal development. *City Environ. Interact.* **19**, 100105 (2023).
37. Li, X., Stringer, L. C. & Dallimer, M. The impacts of urbanisation and climate change on the urban thermal environment in Africa. *Climate* **10**, 164 (2022).
38. Pasquini, L., Van Aardenne, L., Godsmark, C. N., Lee, J. & Jack, C. Emerging climate change-related public health challenges in Africa: A case study of the heat-health vulnerability of informal settlement residents in Dar es Salaam, Tanzania. *Sci. Total Environ.* **747**, 141355 (2020).
39. Kiribou, R. et al. Urban climate resilience in Africa: A review of nature-based solution in African cities' adaptation plans. *Discov. Sustain.* **5**, 94 (2024).
40. Anbazu, J. & Antwi, N. S. Nexus between heat and air pollution in urban areas and the role of resilience planning in mitigating these threats. *Adv. Environ. Eng. Res.* **04**, 047 (2023).
41. Mbandi, A. M. et al. Assessment of the impact of road transport policies on air pollution and greenhouse gas emissions in Kenya. *Energy Strategy Rev.* **49**, 101120 (2023).
42. Okello, G. et al. Air quality management strategies in africa: A scoping review of the content, context, co-benefits and unintended consequences. *Environ. Int.* **171**, 107709 (2023).
43. Wells, C. D., Kasoar, M., Ezzati, M. & Voulgarakis, A. Significant human health co-benefits of mitigating African emissions. *Atmos. Chem. Phys.* **24**, 1025–1039 (2024).
44. Akomolafe, B., Clarke, A. & Ayambire, R. Climate change mitigation perspectives from Sub-Saharan Africa: The technical pathways to deep decarbonization at the City level. *Atmosphere* **15**, 1190 (2024).
45. Perkins, S. E. & Alexander, L. V. On the measurement of heat waves. *J. Clim.* **26**, 4500–4517 (2013).
46. Twinomuhangi, R. et al. Perceptions and vulnerability to climate change among the urban poor in Kampala City. *Uganda Reg. Environ. Change* **21**, 39 (2021).
47. Malings, C. et al. Development of a general calibration model and long-term performance evaluation of low-cost sensors forair pollutant gas monitoring. *Atmospheric Meas. Tech.* **12**, 903–920 (2019).
48. Meehl, G. A. et al. An Introduction to Trends in Extreme Weather and Climate Events: Observations, SocioeconomicImpacts, Terrestrial Ecological Impacts, and Model Projections*. *Bull. Am. Meteorol. Soc.* **81**, 413–416 (2000).
49. Twinomuhangi, R. et al. Perceptions and vulnerability to climate change among the urban poor in Kampala City, *Uganda.Reg. Environ. Change* **21**, 39 (2021).
50. Ha, P.-T. et al. Heatwaves in Vietnam: Characteristics and relationship with large-scale climate drivers. *Int. J. Climatol.***43**,123–140 (2024).

Acknowledgements
We acknowledge the air quality data that the Rwanda Environmental Management Authority provided.

Author contributions
E.K and A.S contributed equally to the study's conceptualization, methodology, data analysis, manuscript review, and editing.

Declarations

Competing interests
The authors declare no competing interests.

Additional information
Correspondence and requests for materials should be addressed to E.K.

Reprints and permissions information is available at www.nature.com/reprints.

Publisher's note Springer Nature remains neutral with regard to jurisdictional claims in published maps and institutional affiliations.